

Characterization of CMOS compatible, waveguide coupled leaky-mode photodetectors

Guangwei Yuan, *Student Member, IEEE*, Robert Pownall, *Student Member, IEEE*, Phil Nikkel, Charles Thangaraj, Thomas W. Chen and Kevin L. Lear, *Member, IEEE*

Abstract—Near-field scanning optical microscopy has been employed for the first time to analyze integrated photodetectors. Waveguide coupled, leaky-mode, polysilicon, metal-semiconductor-metal (MSM) photodiodes fabricated in commercial complementary-metal-oxide-semiconductor (CMOS) technology for on-chip optical interconnects exhibit a measured effective absorption coefficient of 0.67 dB/ μm allowing a 10 μm long detector to absorb 83% of the light in the waveguide with an estimated responsivity of 0.35 A/W at 654 nm. The measured effective absorption coefficient is in good agreement with effective index mode overlap calculations.

Index Terms— NSOM, waveguide coupled leaky mode photodetector, silicon integrated photonics

I. INTRODUCTION

RESEARCH in silicon integrated photonics is not only addressing possible solutions for optical sources, but also approaches for fabricating integrated waveguide and detector systems compatible with conventional complementary-metal-oxide-semiconductor (CMOS) processes. For example, this letter reports work that is part of a project to develop an optical clock distribution system for high-end processors implemented in commercial CMOS technology as a platform for on-chip optical interconnect studies[1]. To minimize barriers to adoption of this technology, only materials already present in CMOS chips are being used to implement the necessary components. In particular, waveguide cores are constructed from silicon nitride used for interconnect metal encapsulation; dielectrics used between metal layers serve as the cladding; and polysilicon films typically used for resistors or gates are adapted for photodetectors. The result is a monolithic, planar, on-chip interconnect technology that can be positioned at various levels in the backend metal stack. For optical clock distribution, an off-chip optical source, perhaps a low-jitter mode-locked laser diode, would be used. CMOS chips containing functioning optical waveguide H-trees and polysilicon photodiodes have been fabricated. This letter

focuses on characterization and modeling of the waveguide coupled leaky-mode detector that demonstrate high power absorption in good agreement with simulations.

A variety of CMOS compatible waveguide coupled photodiode structures have been investigated in the past. Hilleringmann and Goser [2] previously demonstrated waveguide coupled crystalline silicon, p-n photodiodes where the light was directed into a detector in the silicon substrate by three methods including leaky-mode coupling. Their best-observed leaky-mode coupling efficiency was approximately 1.5% for 25 μm long photodiodes corresponding to an effective absorption coefficient of 2.6×10^{-3} dB/ μm . They attributed the low coupling to a 700 nm thick low index layer between the waveguide core and silicon. Nathan *et al* [3] reported quantitative results of light coupling from 12 μm thick, 20 μm wide SU8 multimode waveguides into silicon p-n photodiodes in monolithically integrated structures. The leaky-mode effective absorption coefficients, which they referred to as overlap attenuation, ranged from a minimum of 2.2×10^{-3} dB/ μm to a maximum of 3.05×10^{-3} dB/ μm , somewhat exceeding all of the other results they reviewed except for those of Baba and Kokobun [4]. The latter authors coupled an optical waveguide with a SiO₂ core to a silicon p-n photodiode, achieving effective absorption coefficients of up to 0.027 dB/ μm with an AR coating and 0.001 dB/ μm without an AR coating.

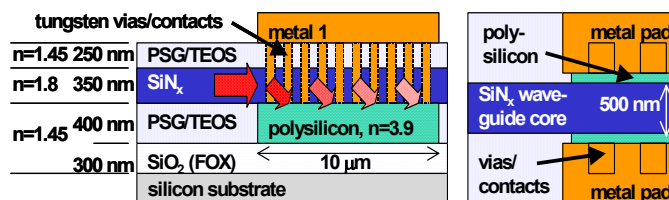


Fig. 1. Cross-sectional (left) and top view (right) diagrams of the waveguide and photodetector.

In comparison to the previous work, our photodetector approach adopts leaky mode coupling from a single-mode, 0.35 μm thick and 0.5 μm wide SiN_x core in direct contact with an undoped polysilicon (p-Si) layer as shown in Figure 1. Details of fabrication will be published elsewhere. The resulting effective absorption coefficient is improved to 0.67 dB/ μm allowing a relatively short 10 μm long photodetector to absorb 83% of the incident power as determined via near-field scanning optical microscopy (NSOM) presented in

Manuscript received March 2, 2006. This work was supported by NSF under grant number ECS-0323493 and by NIH via grant EB00726. G. Yuan, R. Pownall, C. Thangaraj, T. W. Chen and K. L. Lear are with Department of Electrical and Computer Engineering, Colorado State University, Fort Collins, CO, 80523 USA. (Corresponding author phone: 970-491-0718; fax: 970-491-2249; e-mail: klear@engr.colostate.edu).

Phil Nikkel is with Avago Technologies, 4380 Ziegler Road, Fort Collins, CO 80526 USA

Section III. Simple mode overlap calculations of the effective absorption coefficient presented in the next section are in good agreement with the NSOM measurements.

II. MODAL CALCULATIONS

One-dimensional (1-D), effective-index mode calculations provide insight into the operation of the device and NSOM observations. To begin, the effective indices of both the 0.5 μm wide SiN_x ($n=1.80$) waveguide core and the 2.3 μm wide p-Si ($n=3.85+i0.038$) detector, both clad by SiO_2 ($n=1.45$, equivalent to phosphosilicate glass, PSG), were calculated for $\lambda=654$ nm considering only the transverse index variation parallel to the substrate. The extinction coefficient for p-Si was obtained from thin film measurements [5]. The resulting effective indices for the laterally confined SiN_x ($n_{\text{eff}}=1.71$) and p-Si ($n_{\text{eff}}=3.809+i0.0384$) were then used for vertical solutions of the modes using a one-dimensional numerical solution with absorbing boundary conditions positioned 1.0 μm into the air and substrate. Outside the detector region, there are one transverse electric (TE) and one transverse magnetic (TM) modes bound to the SiN_x core. The TM mode's lower confinement factor in the waveguide region results in high relative loss due to substrate absorption and surface scattering in the H-tree leading to the detectors so that only TE modes are considered near the detector.

TABLE I
MODE PARAMETERS

Mode	a^2 , overlap	n_{eff} of mode	α_{eff} (dB/ μm)	E_{surf} (norm.)
Incident mode without p-Si	1	1.62	$<10^{-3}$	1
Bound detector modes ($n_{\text{eff}} > 1.71$)	0.048	$3.74 + i 0.039$	3.3	7.1×10^{-9}
	0.031	$3.54 + i 0.040$	3.4	1.4×10^{-8}
	0.028	$3.17 + i 0.043$	3.6	2.1×10^{-7}
	0.030	$2.60 + i 0.049$	4.1	1.4×10^{-5}
	0.218	$1.76 + i 0.048$	4.0	6.1×10^{-2}
Leaky wave- guide mode ($1.71 > n_{\text{eff}} > 1.45$)	0.60	$1.54 +$ $i 0.0081$	0.68	1.5
Radiation modes ($n_{\text{eff}} < 1.45$)	0.021	$1.24 +$ $i 0.0062$	0.52	1.3

Table I. Modes obtained as solutions to structure shown in Fig. 1. Only the primary radiation mode is listed.

Mode parameters determined from the effective index calculations reveal the factors responsible for the detector's strong optical absorption. The incident TE mode in the waveguide before the p-Si is projected onto a variety of TE modes bound to the p-Si, leaking from the SiN_x core into the p-Si, and radiating into the SiO_2 . The effective indices, n_{eff} , and associated effective absorption coefficients, α_{eff} , of all of these modes are listed in Table I. The distribution of the incident power into each mode is given in terms of the field overlap, a , with the incident mode. The majority, 60%, of the incident power is projected into a mode primarily confined to the SiN_x but leaking into the p-Si at a rate that gives an effective absorption coefficient of 0.68 dB/ μm , a value equal to 21% of the bulk p-Si absorption coefficient. Most of the remaining power, 35.5%, of that incident, is directly coupled into five modes bound to the high index p-Si detector and

therefore rapidly absorbed. The other 4.5% of the incident power is transferred to radiation modes free to propagate in the SiO_2 . The table also lists normalized E-field strengths at the SiO_2 /air surface probed by the NSOM, including the mode overlap factor. Only the leaky waveguide mode and first radiation mode have significant surface strength. 2-D beam propagation method simulations yield modal effective indices within 2% of the simple 1-D calculations except for the imaginary part for the leaky and radiation modes.

III. MEASUREMENTS

The longitudinal dependence of the optical field intensity was measured using NSOM in order to determine the attenuation as well as the initial relative strength of modes observed in experimental structures. Previously published experimental methods for determining the effective absorption coefficient without varying the physical lengths rely on measuring the decay in scattered light, either by imaging the detector region or scanning a fiber over it [6], similar to the common methods for quantifying waveguide loss. Methods relying on scattering to characterize complex waveguide and detector structures are subject to uncertainties about the relative amount of scattering from the various interfaces. Further, since the strength of scattering can be substantially different in regions with and without the detector materials or coupler gratings, related reports have not attempted to quantify the initial intensity of leaky modes relative to the incident waveguide mode but assumed complete coupling to the desired leaky mode [6]. The lack of comparative intensities before and in the detector region prevents experimental evaluation of mode coupling efficiencies associated with calculated overlaps. Another advantage of NSOM over far-field fiber scanning and typical scatter imaging implementations is the resolution it provides. This resolution can be important, for example, to verify the transverse mode profile or to observe mode beating phenomena as discussed below.

A Witec Alpha-SNOM in contact mode measured the optical intensity at the upper PSG/air interface immediately before and above the detector. The same equipment and method have been used earlier to study prototype sensors [7] and waveguide bends [8] but without the thin upper cladding employed here. Fig 2(a) illustrates a false color plot of the measured light intensity over a 10 $\mu\text{m} \times 21.5 \mu\text{m}$ scanned area on the sample surface. The image clearly shows a strong intensity decrease in the detector region where the light is either absorbed or scattered due to the polysilicon layer. In the waveguide before the detector, a Gaussian shaped optical field profile is observed, which corresponds to the guided fundamental TE mode. The measured intensity distribution along the centerline of the waveguide is presented on a log scale in Fig. 2(b) clearly showing oscillations about an average exponential decay. Similar mode beating between leaky and guided modes was observed in stepped waveguide structures used to evaluate a sensor concept [7].

Least squares fitting to the centerline intensity and its average in the detector region provide measured values for α_{eff} and beat length. The slope of the average intensity gives a

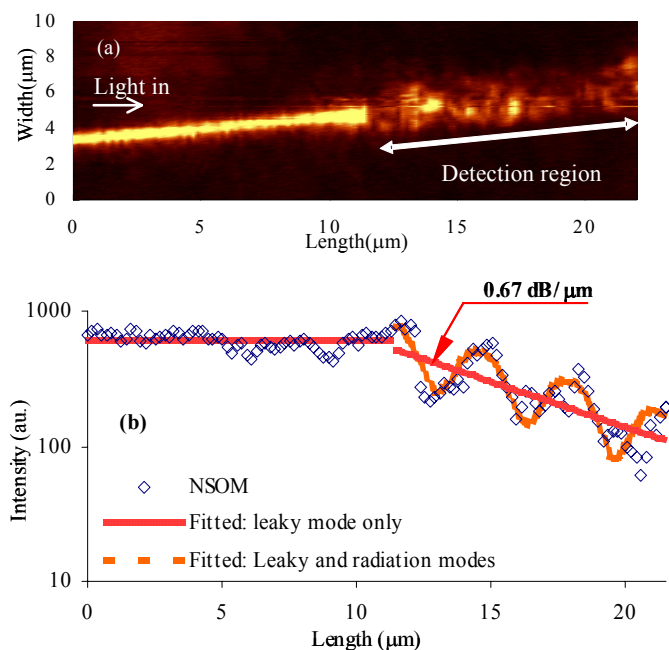


Fig. 2. (a) Near-field image of the measured light intensity over a $10 \mu\text{m} \times 21.5 \mu\text{m}$ scanned area on the sample surface. Note that the horizontal and vertical scales are different. (b) Intensity distribution on the waveguide and detector centerline from measurements (diamonds), fit to leaky and radiation modes (dashed), and fit to only the leaky mode (solid).

measured $\alpha_{\text{eff}} = 0.67 \text{ dB}/\mu\text{m}$ in excellent agreement with the predicted value of $0.68 \text{ dB}/\mu\text{m}$. However, the measured beat length is $3.4 \mu\text{m}$ while the predicted one is $\lambda/(1.54-1.24)=2.2 \mu\text{m}$, and the initial average surface intensity in the detector is observed to drop while the calculations predict an increase by 2.25. Further investigation is required to understand the impact of the 3-D nature of the modes and NSOM coupling dependence on modal properties to resolve these discrepancies. The measured $\alpha_{\text{eff}} = 0.67 \text{ dB}/\mu\text{m}$ is the largest value published to date for a silicon detector and corresponds to 79% power transfer from the leaky mode to the detector. Including the effect of overlap projection and the modes bound to the p-Si indicates that 83% of the incident power is absorbed by the $10 \mu\text{m}$ long p-Si detector. Similar calculations at $\lambda=850 \text{ nm}$ predict that 70% of the power would be absorbed at that longer wavelength.

When biased, the photodetectors operated as expected and demonstrated an excellent on/off ratio across a broad bias voltage range. The measured DC photocurrent and dark current of a $10 \mu\text{m}$ long photodetector with $1.14 \mu\text{m}$ contact spacing across a $0.5 \mu\text{m}$ wide waveguide is shown as a function of bias in Figure 3. The mean photocurrent-to-dark-current ratio exceeds 500 for biases above 2 V. The optical power at 654 nm carried to each detector after splitting and routing in an H-tree structure is estimated to be $1.7 \mu\text{W}$. The $0.6 \mu\text{A}$ photocurrent at 10 V bias voltage corresponds to a responsivity of 0.35 A/W and quantum efficiency of 67%. The difference between the actual quantum efficiency and the 83% power absorption in the p-Si can be attributed to recombination at grain boundaries.

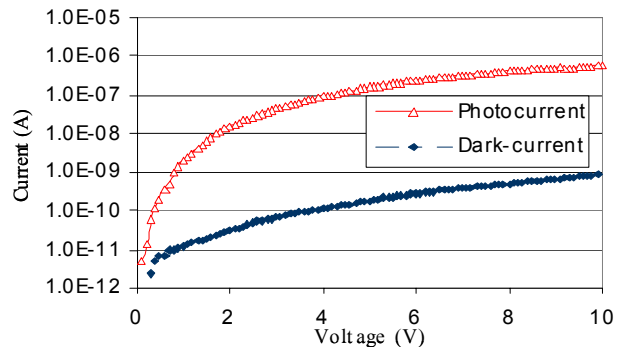


Fig. 3. Dark current (filled diamonds) and photocurrent (open triangles) of a leaky-mode p-Si metal-semiconductor-metal (MSM) photodiode due to an estimated $1.7 \mu\text{W}$ of incident power at 654 nm .

IV. SUMMARY

Near-field scanning optical microscopy (NSOM) has been employed for the first time to determine the effective absorption coefficient of a waveguide coupled leaky-mode polysilicon photodetector. A very high value of $0.67 \text{ dB}/\mu\text{m}$ was obtained for the p-Si structure at $\lambda=654 \text{ nm}$ indicating that a relatively short $10 \mu\text{m}$ long photodetector absorbs 79% of the leaky mode power and 83% of the incident power in the waveguide. An estimated experimental responsivity of 0.35 A/W at 10 V is in reasonable agreement with the absorption characterization. Modal overlap calculations based on one-dimensional numerical mode solutions in the effective index approximation provided good predictions of the expected performance. A complete optical clock distribution system including integrated receivers is currently being fabricated in a commercial CMOS process and will be reported later.

REFERENCES

- [1] A.M. Raza, G.W. Yuan, C. Thangaraj, T. Chen, K.L. Lear, "Waveguide coupled CMOS photodetector for on-chip optical interconnects," *The 17th Annual Meeting of the IEEE LEOS*, vol.1, pp.152-153, 2004.
- [2] U. Hilleringmann and K. Goser, "Optoelectronic System Integration on Silicon: Waveguides, photodetectors, and VLSI CMOS circuits on One Chip," *IEEE Transactions on Electron Devices*, vol. 42, No. 5, pp. 841-846, May 1995.
- [3] M. Nathan, O. Levy, I. Goldfarb, A. Ruzin, "Monolithic coupling of a SU8 waveguide to a silicon photodiode," *Journal of Applied Physics*, vol. 94, pp. 7932-7934. Dec. 2003.
- [4] T. Baba and Y. Kokubun, "High efficiency light coupling from antiresonant reflecting optical waveguide to integrated photodetector using an antireflecting layer," *Appl. Opt.*, vol. 29, pp. 2781-2792, Jun. 1990
- [5] A.M. Raza, M.S. Thesis, Colorado State University, 2005.
- [6] N. M. Jokerst, T. K. Gaylord, E. Glytsis, M. A. Brooke, S. Cho, T. Nonaka, T. Suzuki, D. L. Geddis, J. Shin, R. Villalaz, J. Hall, A. Chellappa, and M. Vrazel, "Planar Lightwave Integrated Circuits With Embedded Actives for Board and Substrate Level Optical Signal Distribution," *IEEE Transactions on Advanced Packaging*, vol. 27, pp. 376-385, May. 2004.
- [7] G. W. Yuan, M.D. Stephens, D.S. Dandy, K. L. Lear, "Direct imaging of transient interference in a single-mode waveguide using near-field scanning optical microscopy," *IEEE Photonics Technology Letters*, vol 17, pp.2382 - 2384, Nov. 2005.
- [8] G. W. Yuan, M.D. Stephens, D.S. Dandy, K. L. Lear, "Characterization of a 90 degrees waveguide bend using near-field scanning optical microscopy," *Applied Physics Letters*, vol. 87, Art. No. 191107 Oct. 2005.